

State-specific Photochemistry of Molecular Adsorbates on Surfaces

Photon induced surface reactions of molecular adsorbates on surfaces have received considerable attention, because such chemistry plays an important role in application to photon-assisted chemical vapor deposition and fabrication of microelectronic devices. As the dimensions of electronic devices get smaller into the nanometer range, the required photon wavelength for the surface photochemistry becomes shorter, for instance, from UV in the conventional photolithography into the vacuum UV and X-ray regime. Obviously, understanding of the X-ray excited molecular processes on surfaces is essential for the development of the evolving technology.

With tunable-energy synchrotron radiations in the X-ray region, it is possible to excite selectively the specific atom or specific site in a molecule. Besides, the core electrons of a specific element in a molecule can be selectively excited into the specific valence orbitals and Rydberg states below the ionization threshold. As illuminated in Fig. 1, the bond-selective photoexcitation and subsequent cleavage of the specific chemical bond of molecules via core-level excitation using synchrotron radiation have been a topic of extensive study. In the past decade, the site-specific fragmentation via core-level excitation has been observed in the gas phase, adsorbed molecules, and polymers. The site-selective photofragmentation of molecular adsorbates on surfaces provides a new possibility to synthesize new materials. For example, excitations of Br 3d core electrons to the $\sigma^*(\text{C-Br})$ orbital in CH_3Br and $\text{C}_2\text{H}_5\text{Br}$ have been shown to enhance C-Br bond cleavage as compared to C-H or C-C. However, for $\text{Si}_2(\text{CH}_3)_6$, no selectivity of bond cleavage has been found after excitations to various resonances at the Si 2p edges. For $\text{Fe}(\text{CO})_2(\text{NO})_2$, no difference has been observed following excitation of the C 1s and N 1s edges. Till now, the mechanisms of bond-selective fragmentation of molecules via core-level excitation

are not fully understood. In addition, the fragmented ions observed in the previous studies were exclusively positive ions. The study of negative-ion desorption of molecular adsorbates via inner-shell excitation is in its infancy. It has been shown that there exist some highly excited states near or above the double ionization threshold energies in gas-phase molecules, such as SO_2 and CO. However, very little research has been conducted to study these highly excited states and their roles on ion desorption processes for adsorbates on surfaces.

The comprehensive understanding of the interaction of Cl-containing compounds (SiCl_4 , Si_2Cl_6 , CCl_4 , *etc.*) with silicon is of substantial importance in the semiconductor industry. In the present study, by combining the photon-stimulated ion desorption (PSID) spectra (positive and negative ions), resonant photoemission spectra, X-ray absorption spectra, and ion energy distribution measurements, the mechanisms of state-selective fragmentation for SiCl_4 adsorbed on Si(100) at ~ 90 K following the Cl 2p and Si 2p core-level excitations to various resonances are characterized.

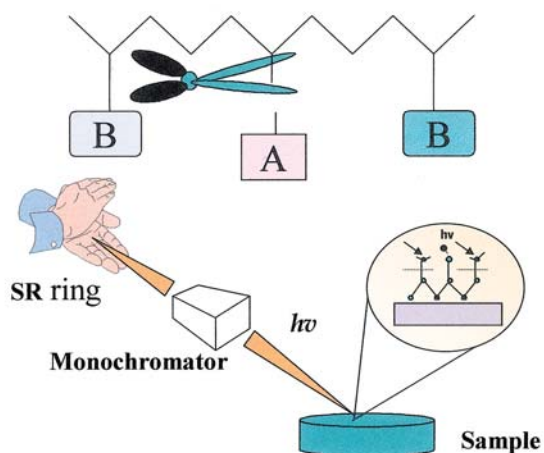


Fig. 1: The bond-selective photoexcitation and subsequent cleavage of the specific chemical bond of molecules using synchrotron radiation.

The PSID spectra of SiCl^+ , SiCl_2^+ , SiCl_3^+ , Si^+ , and Cl^+ from SiCl_4 adsorbed on $\text{Si}(100)$ at ~ 90 K with multilayer coverage (> 100 -L exposure) at the Cl 2p edge in the photon energy range, 198–220 eV, are reproduced in Fig. 2(a). The Cl L_{23} -edge X-ray absorption spectrum for condensed SiCl_4 measured by the total electron yield (TEY) mode is also displayed for comparison. As shown, the X-ray absorption spectrum for condensed SiCl_4 exhibits several pronounced pre-edge features in the vicinity of Cl 2p edges. The absorption peaks labeled 1, 1', and 2, 2' in Fig. 2(a) are separated by an energy of ~ 1.6 eV, which is equivalent to the spin-orbit splitting of Cl $2p_{3/2}$ and Cl $2p_{1/2}$. Based on multiple scattering $X\alpha$ calculations of SiCl_4 , the absorption peaks labeled 1 and 1' are assigned to the transition, $\text{Cl } 2p \rightarrow 8a_1^*$. The features labeled 2 and 2' correspond to the $\text{Cl } 2p \rightarrow$

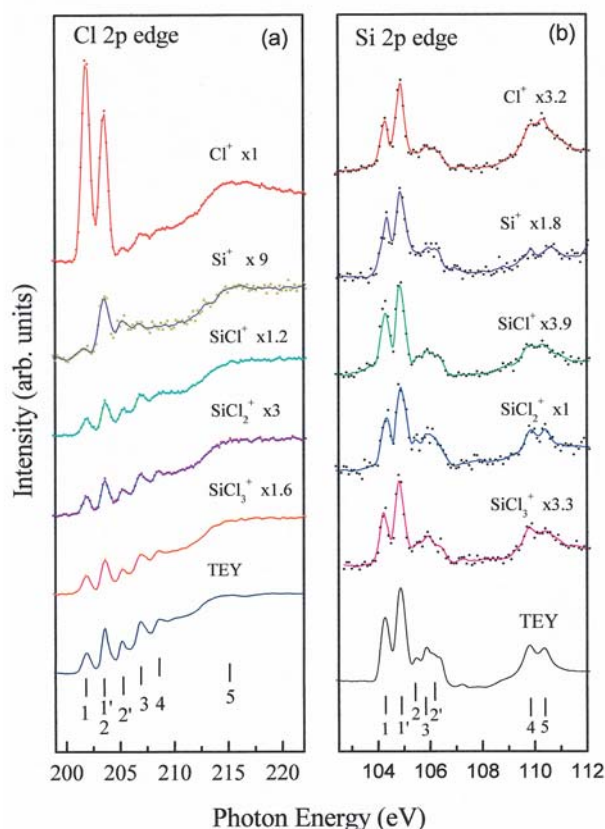


Fig. 2: (a) PSID spectra of Cl^+ , Si^+ , SiCl^+ , SiCl_2^+ , and SiCl_3^+ for condensed SiCl_4 (> 100 -L exposure) along with the Cl L-edge TEY spectrum via the Cl 2p core-level excitation. (b) PSID spectra of Cl^+ , Si^+ , SiCl^+ , SiCl_2^+ , and SiCl_3^+ , along with the TEY spectrum, from solid SiCl_4 following the Si 2p core-level excitation. For details of the assignments, see the text.

$9t_2^*$ excitations. Excitations to the Rydberg states are responsible for the absorption peaks labeled as 3 and 4. The broad band at ~ 216 eV labeled as 5 is ascribed to the shape resonance.

As noted from Fig. 2(a), the PSID spectra of SiCl^+ , SiCl_2^+ , SiCl_3^+ and Si^+ show a close resemblance to the Cl L_{23} -edge X-ray absorption spectrum of solid SiCl_4 . In contrast, the Cl^+ PSID spectrum exhibits a clear dissimilarity from the Cl L_{23} -edge X-ray absorption spectrum. The transition, $\text{Cl } 2p \rightarrow 8a_1^*$, leads to a significant enhancement in the Cl^+ desorption yield when compared to the transitions, $\text{Cl } 2p \rightarrow 9t_2^*$ and $\text{Cl } 2p \rightarrow$ Rydberg states. Even though these states are assigned to transitions from the same atomic site, there is a significant difference in efficiency for producing various ions. This infers that the characters of core-excited states play a vital role in the ion desorption processes.

In Fig. 2(b), the PSID spectra of Cl^+ , Si^+ , SiCl^+ , SiCl_2^+ , and SiCl_3^+ , along with the TEY spectrum, from solid SiCl_4 via the Si 2p core-level excitation are displayed in the incident photon energy range of 101–112 eV. The high-intensity doublet peaks labeled 1 and 1' were ascribed to transitions from the $\text{Si}(^2P_{3/2,1/2})$ initial states to the $8a_1^*$ state. The next doublet structures labeled 2 and 2' were assigned to excitations to the $9t_2^*$ state. As noted, the observed structures in the PSID spectra of various desorbed ions correspond to the structure in the Si L-edge TEY spectrum.

It is intriguing to compare the ion desorption of condensed SiCl_4 following the Si 2p and Cl 2p core-level excitations. The yields for various desorbed ions from solid SiCl_4 were observed with almost comparable intensities at the Si 2p edge. For the Cl 2p core-level excitation, the ion yields of SiCl^+ , SiCl_2^+ , and SiCl_3^+ were found to be comparable in magnitude, while the Si^+ desorption exhibits a relatively weak yield. The $\text{Cl } 2p \rightarrow 8a_1^*$ excitation induces a significant enhancement of the Cl^+ yield, while the $\text{Si } 2p \rightarrow 8a_1^*$ excitation leads to a scarce enhancement of the Cl^+ yield.

Based on resonant photoemission measurements, the spectator Auger and normal Auger transitions were the dominant decay channels for the excited Cl 2p and Si 2p core holes of condensed SiCl_4 , producing excited states with

multiple holes in the valence orbitals. Accordingly, a close resemblance of the PSID spectra to the Cl L-edge (or Si L-edge) TEY spectrum of solid SiCl_4 , as shown in Fig. 2, is attributed to the Auger decay of core-excited states and subsequent Coulomb explosion of multi-valence-hole final states, which was called the Auger-initiated desorption (AID) mechanism. However, the observed dissimilarity between the Cl L-edge TEY spectrum and the Cl^+ PSID spectrum suggests that there exist additional channels for Cl^+ desorption in solid SiCl_4 .

In Fig. 3(a), the Cl^+ ion energy distributions of SiCl_4 adsorbed on Si(100) at ~ 90 K with multi-layer coverage following the Cl 2p core-level excitations are reported. As noted, the Cl^+ ion energy distributions via the Cl 2p $\rightarrow 8a_1^*$ excitation are shifted to higher energy (~ 0.3 eV) compared to those via the Cl 2p $\rightarrow 9t_2^*$ and Cl 2p \rightarrow shape resonance excitations. Based on the $Z+1$ equivalent core model, after excitations of Cl 2p

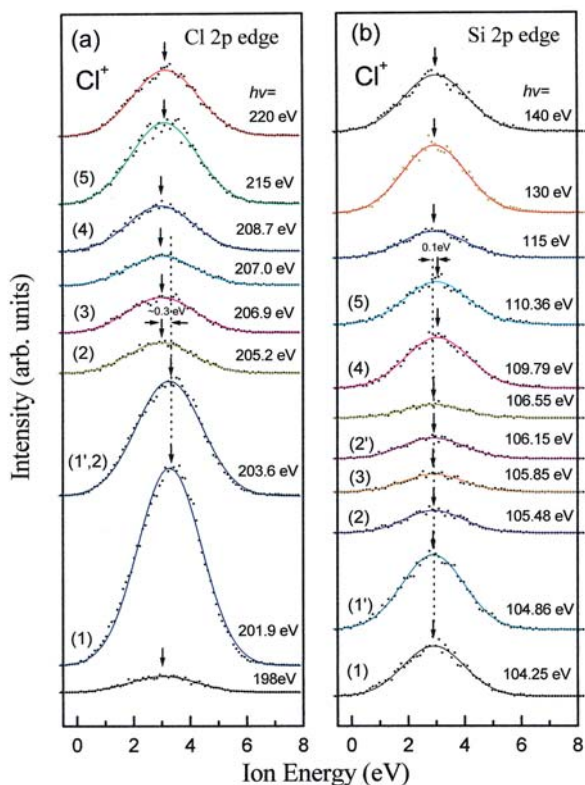


Fig. 3: Cl^+ ion energy distributions for SiCl_4 adsorbed on Si(100) at ~ 90 K (30-L exposure) following the (a) Cl 2p and (b) Si 2p core-level excitations. The photon energy used for the excitation is indicated in each spectrum. The number indicated in each spectrum corresponds to absorption peak marked in the TEY spectrum in Fig. 2.

core electrons into the $8a_1^*$ orbital in SiCl_4 , the core equivalent molecule is $\text{Cl}_3\text{Si-Ar}$ in its fundamental state. Obviously, this core-excited state is expected to present a strongly repulsive potential surface. In contrast, the $9t_2^*$ and Rydberg orbitals are more diffuse and the corresponding core-excited states may be bound in the Franck-Condon region, similar to the core ionized molecules. Thus, the potential surface at the $\text{Cl}(2p)^{-1}8a_1^*$ resonance is expected to be much steeper than that at the $\text{Cl}(2p)^{-1}9t_2^*$ resonance. Accordingly, the excess kinetic energy for desorbed Cl^+ at the $\text{Cl}(2p)^{-1}8a_1^*$ resonance is higher than that at the $\text{Cl}(2p)^{-1}9t_2^*$ resonance, as evidenced in Fig. 2(a). It is clear that, due to higher ion kinetic energy and consequently lower ion reneutralization rates, the Cl^+ yield via the Cl 2p $\rightarrow 8a_1^*$ excitation is significantly enhanced.

Fig. 3(b) presents the Cl^+ ion energy distributions of condensed SiCl_4 in the vicinity of Si 2p edge. As noted, the Cl^+ ion energy distributions remain nearly constant via the Si 2p core-level excitation to various valence states. The steepness of a potential surface of an excited state is correlated closely with the peak width in an absorption spectrum. The steeper the slope in the Franck-Condon region, the broader the absorption peak. As noted from Fig. 2, the $8a_1^*$ resonance at the Si 2p edge in the X-ray absorption spectrum is significantly narrower than that at the Cl 2p edge (FWHM of 0.33 eV for the Si 2p edge and that of 0.83 eV for the Cl 2p edge), corresponding to different lifetimes or Franck-Condon factors of the corresponding core-excited states. The peak envelope exceeds the core-hole lifetime broadening and the energy resolution of beamlines (0.1 eV at the Si 2p edge and 0.3 eV at the Cl 2p edge). The variation of peak width thus might reflect the different slopes of potential surfaces in the Franck-Condon region of the corresponding core-excited states. It is therefore expected that the potential surface of the $\text{Si}(2p)^{-1}8a_1^*$ core-excited state is less repulsive than that of the $\text{Cl}(2p)^{-1}8a_1^*$ resonance. As shown in Fig. 3, the Cl^+ ion energy distribution via the Si 2p excitation shows a lower energy (0.3-0.4 eV) as compared to that at the $\text{Cl}(2p)^{-1}8a_1^*$ resonance. As a result, the Si 2p $\rightarrow 8a_1^*$ excitation gives rise to a scarce enhancement of the Cl^+

yield. These results provide possible explanations why bond-selective fragmentation of molecules via core-level excitation was not observed in some systems.

Unlike the positive-ion desorption, the Cl^- was the only ion predominantly observed in the negative-ion desorption of $\text{SiCl}_4/\text{Si}(100)$ following the Cl 2p core-level excitation. In order to get more insight into the mechanism of negative-ion desorption, the Cl^- yield was measured as a function of SiCl_4 exposure on Si(100) at ~ 90 K, as presented in Fig. 4(a). The surface coverage was determined by thermal desorption spectroscopy (TDS). The TDS spectra from $\text{SiCl}_4/\text{Si}(100)$ show a single molecular desorption peak at ~ 139 K with an exposure of 5 L or less. Above 5-L exposure, an additional peak starts to appear at a lower temper-

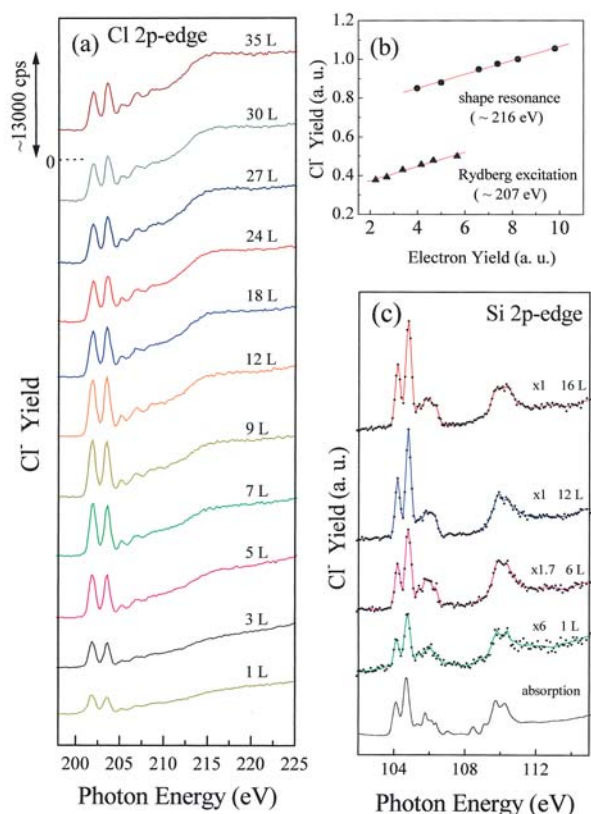


Fig. 4 (a) Cl^- yield spectra for SiCl_4 on $\text{Si}(100)$ at ~ 90 K with variable exposures in the vicinity of Cl 2p edge. (b) The Cl^- yields at the shape resonance and Rydberg excitations versus the corresponding total electron yields for the respective SiCl_4 exposures (12-L exposure and more). (c) Cl^- yield spectra from $\text{SiCl}_4/\text{Si}(100)$ at ~ 90 K with variable exposures near the Si 2p edge. Si L-edge X-ray absorption spectrum of gaseous SiCl_4 is shown at the bottom of this Figure for comparison.

ature of ~ 124 K and its intensity increases with increasing exposure. Thus, 5-L exposure of SiCl_4 on $\text{Si}(100)$ corresponds to one monolayer (ML).

As noted from Fig. 4(a), the Cl^- yield spectra exhibit several interesting features. There is a significant enhancement in Cl^- yield at the $8a_1^*$ resonance with SiCl_4 exposures. Besides, the Cl^- yield at the $8a_1^*$ resonance increased up to 12-L exposure and then decreased slowly beyond 12-L exposure of SiCl_4 on $\text{Si}(100)$. In contrast, the Cl^- yield at the shape resonance increased drastically up to 5-L exposure and increased slowly after 12-L exposure of SiCl_4 on $\text{Si}(100)$. To corroborate the Cl^- yield, the corresponding total electron yield is plotted against the Cl^- yield at the shape resonance and Rydberg excitations for the respective SiCl_4 exposure (for 12-L exposure and more) in Fig. 4(b). As shown, the Cl^- yields at both shape resonance and Rydberg excitations show linear dependences with the electron yield. This implies that the possible desorption process of atomic fragment Cl^- from $\text{SiCl}_4/\text{Si}(100)$ is likely due to dissociative attachment on molecules of secondary electrons created by photoabsorption of molecular adsorbates. This desorption mechanism was called dissociative electron attachment (DEA).

In contrast, the enhancement of Cl^- yield at the $8a_1^*$ resonance is not due to DEA processes, but it originates from unimolecular processes. This is due to the fact that the observed $\text{Cl}(2p_{1/2,3/2})^{-1}8a_1^*$ resonances have the same energy and width among Cl^- yield, positive-ion yield and TEY spectra. One of the possible processes for negative-ion formation by photoexcitation of a molecule is attributed to some highly excited states of the parent ion that predissociate into ion pairs or directly dissociate. Here, we consider that the resonances of SiCl_4 molecules via the Cl 2p core-level excitation can decay by Auger transition to these highly excited states. It has been demonstrated that the intensities of the resonances in the negative-ion spectrum are strongly correlated to the probability of spectator electrons to attach to the electronegative atom during fragmentation of the molecules. From the multiple-scattering $X\alpha$ calculations of SiCl_4 , the spectator electron in the $8a_1^*$ orbital is more localized at the Cl side, while

the $9t_2^*$ orbital is delocalized between Cl and Si atoms. It is thus expected that the Cl $2p \rightarrow 8a_1^*$ excitation leads to an enhancement of Cl⁻ yield, as compared to the Cl $2p \rightarrow 9t_2^*$ and Cl $2p \rightarrow$ Rydberg excitations. This is indeed observed in Fig. 4(a).

If the highly excited states exist, it is reasonably expected that these states can also be populated by Auger decay of Si(2p) core-excited states of SiCl₄. Fig. 4(c) shows the Cl⁻ yield spectra from SiCl₄/Si(100) at ~90 K with variable exposures following the Si 2p core-level excitation, along with the gas-phase X-ray absorption spectrum. As shown, the relative Cl⁻ yields at the Si $2p_{1/2} \rightarrow 8a_1^*$ excitation (~104.8 eV) and the Si $2p_{1/2} \rightarrow 9t_2^*$ excitation (~106.1 eV) show a continuous increase up to 12-L exposure of SiCl₄ on Si(100). The enhancement of Cl⁻ yield at the $8a_1^*$ resonance is clearly observed (particularly for 12-L exposure). This gives evidence in support of the existence of some highly excited states. Similar phenomenon has been found for OPCl₃ (P 2p and Cl 2p edges), Si(CH₃)_{4-n}Cl_n ($n = 1-3$) (Si 2p and Cl 2p edges), SO₂Cl₂, (S 2p and Cl 2p edges), *etc.* The negative ion formation through the highly excited states is thus not specific to the SiCl₄ molecule. It is therefore believed that the present experimental finding is of a general nature.

The present experimental results clearly demonstrate that bond-selective photofragmentation of molecules is brought about by different aspects of the evolution of the electronically excited entity, with contributions from the primary core-excited states, and from the multiply excited valence states arrived at after Auger decay. These results are crucial for understanding the origins of selective fragmentation of molecules following core-level excitation.

Beamlines:

20A1 High Energy SGM beamline
08A1 Low Energy SGM beamline

Experimental Station:

Photoabsorption and photodesorption end station

Authors:

J. M. Chen and K. T. Lu

National Synchrotron Radiation Research Center,
Hsinchu, Taiwan

Publications:

- J. M. Chen and K. T. Lu, Phys. Rev. Letters **86**, 3176 (2001).
- J. M. Chen, K. T. Lu, and J. M. Lee, J. Chem. Phys. **118**, 5087 (2003)

Contact e-mail:

jmchen@nsrrc.org.tw